Cell Stem Cell
Article

# Wip1 Phosphatase Regulates p53-Dependent Apoptosis of Stem Cells and Tumorigenesis in the Mouse Intestine

Oleg N. Demidov,[1,3] Oleg Timofeev,[1,3] Hnin N.Y. Lwin,[1] Calvina Kek,[1] Ettore Appella,[2] and Dmitry V. Bulavin[1,*]
[1] Cell Cycle Control and Tumorigenesis Group, Institute of Molecular and Cell Biology, 61 Biopolis Drive, Proteos 138673, Singapore
[2] Laboratory of Cell Biology, Center for Cancer Research, NCI, NIH, Bethesda, MD 20892, USA
[3] These authors contributed equally to this work.
*Correspondence: dvbulavin@imcb.a-star.edu.sg
DOI 10.1016/j.stem.2007.05.020

## SUMMARY

**Colorectal cancer is one of the major causes of cancer-related deaths. To gain further insights into the mechanisms underlying its development, we investigated the role of Wip1 phosphatase, which is highly expressed in intestinal stem cells, in the mouse model of APC$^{Min}$-driven polyposis. We found that Wip1 removal increased the life span of APC$^{Min}$ mice through a significant suppression of polyp formation. This protection was dependent on the p53 tumor suppressor, which plays a putative role in the regulation of apoptosis of intestinal stem cells. Activation of apoptosis in stem cells of Wip1-deficient mice, but not wild-type APC$^{Min}$ mice, increased when the Wnt pathway was constitutively activated. We propose, therefore, that the Wip1 phosphatase regulates homeostasis of intestinal stem cells. In turn, Wip1 loss suppresses APC$^{Min}$-driven polyposis by lowering the threshold for p53-dependent apoptosis of stem cells, thus preventing their conversion into tumor-initiating stem cells.**

## INTRODUCTION

Colorectal cancer (CRC) is the second largest cause of cancer-related deaths in Western countries. CRC arises as a result of stepwise genetic alterations in specific oncogenes and tumor suppressors. Mutations in the tumor suppressor adenomatosis polyposis coli (APC) gene, a gatekeeper gene in CRC tumorigenesis, occur early in the development of CRC and lead to the stabilization of β-catenin and constitutive activation of Wnt signaling (Polakis, 1997). Much of our current knowledge comes from studies of the hereditary CRC syndrome, familial adenomatous polyposis (FAP). In FAP, individuals develop numerous intestinal adenomas relatively early in life that rapidly progress to carcinomas. In addition, mouse models of CRC continue to make critical contributions to our understanding of the molecular mechanisms underlying this multistage disorder. Mice mutant for APC, similar to the defect in FAP patients and in many sporadic cancers, mimic the rapid development of adenomatous polyps that affects humans with germline inactivation of one *APC* gene (Su et al., 1992). *Apc*$^{Min/+}$ mice have a nonsense mutation at codon 850 in the *Apc* gene that results in a truncated protein product, and these mice are predisposed to form intestinal tumors. In *Apc*$^{Min/+}$ mice, tumors arise as a result of loss of heterozygosity (LOH) at *Apc* as well as through LOH-independent mechanisms (Reitmair et al., 1996).

Accumulating evidence supports a role for stem cells in tumorigenesis, including CRC, and several intestinal stem cell markers are highly expressed in APC$^{Min}$ adenomas and carcinomas (O'Brien et al., 2007; Ricci-Vitiani et al., 2007; Van der Flier et al., 2007). In turn, targeting stem cells during their conversion into cancer stem cells represents a powerful yet unexploited cancer-prevention tool. The problem, however, is in detecting intestinal stem cells and thus analyzing their behavior. Self-renewal and organ development assays are not possible with intestinal stem cells; however, their position within the crypt is well defined (Marshman et al., 2002; Potten and Ellis, 2006). There are 4–6 stem cells at the crypt base (positions 4–6) that normally divide once a day, producing a pool of proliferative progenitors that differentiate while moving up the crypt in a continuous wave to be shed after a total lifetime of about 5–7 days (Potten and Ellis, 2006). One of the remarkable features of intestinal stem cells is that, despite their large number and rapid rate of cell division, these cells rarely acquire the age-related genetic defects associated with cancer induction or show deterioration in functional competence. This observation suggests that intestinal stem cells have evolved protective mechanisms against genetic damage. Among them is the ability of stem cells to selectively sort the old (parental) and new DNA strands when they divide, retaining only parental DNA strands (Potten et al., 2002). This phenomenon is called asymmetric division and ensures that replication-induced errors are excluded from stem cells. Random errors introduced into parental strands (e.g., after exposure to genotoxic agents) trigger a second protective

response, robust p53-dependent stem cell apoptosis (Merritt et al., 1994). Conceivably, alteration of either mechanism could expedite tumorigenesis or, conversely, serve as a powerful cancer-prevention tool.

The Wip1 phosphatase is emerging as a potent regulator of tumorigenesis through its ability to attenuate the activity of several stress-induced kinases (Demidov et al., 2007; Shreeram et al., 2006a; Nannenga et al., 2006; Lu et al., 2005; Fujimoto et al., 2006). We previously found that deletion of Wip1 results in a dramatic delay in the onset of mammary gland tumors and lymphomas in cancer-prone mouse strains (Bulavin et al., 2004; Shreeram et al., 2006b). In turn, $Apc^{Min/+}$ mice have been instrumental in colon cancer studies (Corpet and Pierre, 2003); however, the molecular events involved in neoplasia in CRC have only been partially characterized. We therefore chose this in vivo tumor model to analyze the role of Wip1 in the initiation and progression of intestinal cancer. We found that Wip1 phosphatase modulates $APC^{Min}$-driven polyposis by setting a threshold for p53-dependent apoptosis of stem cells, thus preventing their conversion into tumor-initiating/cancer stem cells.

## RESULTS

### Expression of Wip1 Phosphatase in Mouse Intestine

To determine the distribution of Wip1 in the mouse intestine, we analyzed Wip1 mRNA expression using in situ hybridization and found positively stained cells within the crypt base (Figure 1A and see Figure S2 in the Supplemental Data available with this article online). Analysis of the cell position along the crypt axis indicated that Wip1 mRNA-positive cells were predominantly in position 4 from the crypt base. To further characterize Wip1-expressing cells, we performed an immunohistochemical analysis using a polyclonal antibody to Wip1 (Fujimoto et al., 2006). We found the majority of Wip1-positive cells were in position 4, with the long tail to the right (Figure 1A, right panels).

Stem/early progenitor cells occupy positions 4–6 in the intestine, whereas Paneth cells occupy the first three positions (Potten et al., 2002; Potten and Ellis, 2006). To further characterize Wip1-expressing cells, we used antibodies to phospho-PTEN, a recently identified intestinal stem cell marker (He et al., 2004, 2007). Consistent with previous data (He et al., 2004, 2007), we found that the phospho-PTEN antibody predominantly stained cells in stem cell positions 4–6 from the base of the crypt (Figure 1B and Figure S2). Next, we performed dual immunohistochemical staining of Wip1 and phospho-PTEN and found coexpression of these two markers (Figure 1C).

As has been established in the field, the approach to analyze adult stem cells is to perform label-retaining experiments using either [$^3$H]thymidine or BrdU (Radtke and Clevers, 2005; Potten et al., 2002; Waikel et al., 2001; Welm et al., 2002; Urbanek et al., 2006). In the mouse intestine, label-retaining experiments have been supported by experiments using ionizing radiation (IR), which provides a surrogate repopulation (organ development) test. It has been established that label-retaining cells are the most sensitive cells to IR and that the extent to which these cells are killed by IR is reflected in the intestinal morphology (reviewed in Potten and Ellis, 2006). Furthermore, the death of label-retaining cells affects crypt survival in the mouse intestine. The above data confirm that label-retaining cells are intestinal stem cells. To rigorously test whether Wip1-positive cells are indeed intestinal stem cells, we next carried out juvenile label-retaining experiments using [$^3$H]thymidine (Potten et al., 2002). This protocol labels proliferating cells, including stem cells. In the intestine, almost all labeled cells are removed due to continuous flow up the crypt, where they are shed in the intestinal lumen. Two features of stem cells allow them to retain [$^3$H]thymidine. First, stem cells do not migrate but continue to reside in the intestine and, once labeled, are easy to detect. Second, even when they divide, intestinal stem cells retain the labeled parental strands of DNA, thus preventing [$^3$H]thymidine-labeled DNA from being diluted during multiple rounds of division (Potten et al., 2002). We injected 5- to 6-week-old wild-type mice with 50 μCi [$^3$H]thymidine every 12 hr for 3 days and sacrificed them 3 weeks after the last injection. Consistent with previous reports (Potten et al., 2002; Potten and Ellis, 2006), we found [$^3$H]thymidine-retaining cells predominantly in position 4 from the crypt base (Figure 1D). Subsequent costaining for Wip1 revealed that the majority of [$^3$H]thymidine-retaining cells were positive for Wip1 (Figure 1D, right panel), supporting the idea that Wip1 is specifically expressed in intestinal stem cells.

It is important to emphasize that our data do not exclude the possibility that Wip1-expressing stem cells could be found in the Paneth cell area. As shown in Figures 1A and 1D, about 40% of cells in the Paneth cell compartment retain [$^3$H]thymidine and express Wip1 mRNA. Thus, our data are compatible with the hypothesis that some intestinal stem cells reside in the Paneth area (Bjerknes and Cheng, 2006).

Expression of Wip1 phosphatase after DNA damage is dependent on the p53 tumor suppressor (Choi et al., 2002; Fiscella et al., 1997). To investigate whether intestinal Wip1 expression is regulated through p53, we carried out an immunohistochemical analysis of Wip1 in the intestines of p53 null mice. Compared to wild-type mice, Wip1 was present in p53 null intestines at similar levels and in similar cell positions within the crypt base (Figure 1E). Thus, Wip1 expression is regulated in a p53-independent manner in mouse intestinal stem cells.

### Wip1 Phosphatase Regulates $APC^{Min}$-Induced Polyposis

To understand the potential role of Wip1 in regulating intestinal tumorigenesis and in $Apc^{Min/+}$-driven polyposis in particular, we next carried out real-time PCR analysis of Wip1 mRNA in polyps and compared it with Wip1 mRNA levels in normal intestinal epithelium. Total RNA was purified from intestinal epithelium and microdissected polyps, both obtained from $APC^{Min}$ mice, and

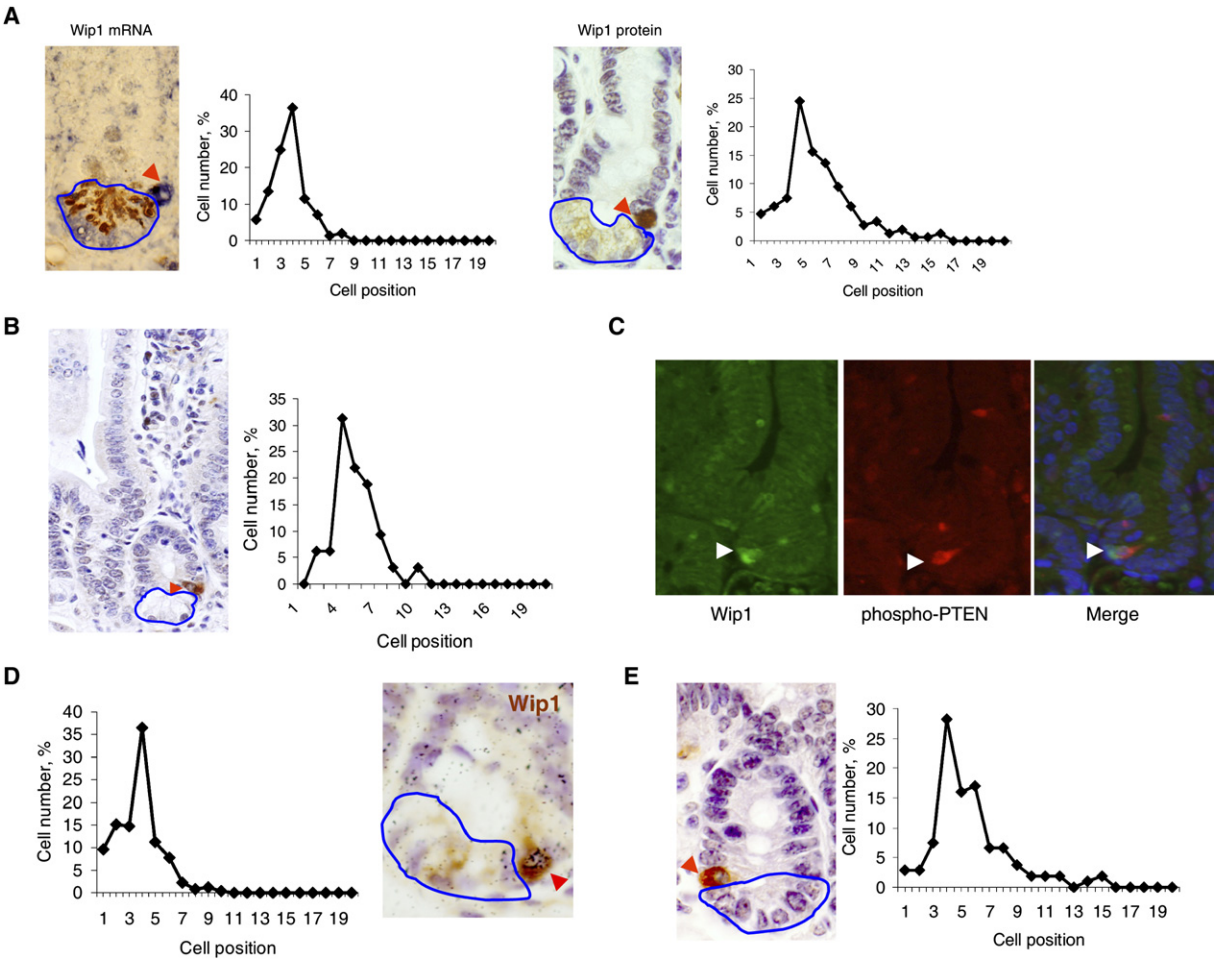


**Figure 1. Wip1 Phosphatase Is Expressed in Intestinal Stem Cells**

(A) Wip1 mRNA and protein expression (shown with arrowheads) was analyzed in intestine sections obtained from wild-type mice using in situ RNA hybridization (left panel) and immunohistochemistry with an antibody to Wip1 (right panel). The Paneth cells were counterstained with an antibody to lysozyme. The number and position of Wip1-positive cells within the crypt base were plotted.

(B) Phospho-PTEN-positive cells were identified using an antibody specific for phospho-PTEN, and the number and position of phospho-PTEN-positive cells (shown with arrowhead) within the crypt base were plotted. The area containing Paneth cells is outlined.

(C) Two consecutive intestine sections were stained for Wip1 (left) or phospho-PTEN (right) and merged. Positively stained cells are shown with arrowheads.

(D) Label-retaining experiments were carried out using juvenile wild-type mice as described in the Experimental Procedures. The position of [$^3$H]thymidine-retaining cells was counted, and slides were counterstained for Wip1 (right panel). Label-retaining cell is shown with arrowhead. The Paneth cell area is outlined.

(E) Wip1 protein expression was analyzed in p53 null mouse intestines, and the number and the position of Wip1-positive cells (shown with arrowhead) within the crypt base were plotted. The area containing Paneth cells is outlined.

used for reverse transcription and subsequent real-time PCR analysis. The level of Wip1 mRNA in polyps was ~5-fold greater than in intestinal epithelium (Figure 2A). The Wip1 mRNA overexpression in polyps of APC$^{Min}$ mice was further confirmed by in situ RNA hybridization (Figure 2B).

It is possible that accumulation of Wip1 in polyps in the course of APC$^{Min}$-driven polyposis is a consequence of cancer progression rather than a contributing factor. To investigate this possibility, *Apc*$^{Min/+}$ mice were crossed with Wip1 null mice, and then we intercrossed *Wip1*$^{+/-}$ mice carrying the *Apc*$^{Min/+}$ allele to yield two genotypes: *Wip1*$^{+/+}$ and *Wip1*$^{-/-}$ mice, all carrying the *Apc*$^{Min/+}$ allele. To investigate tumor onset, we used only littermates from the same parents for all crosses. We found that *Wip1*$^{-/-}$ mice survived longer than wild-type (WT)/*Apc*$^{Min/+}$ mice (Figure 2C) and developed only a few polyps by day 120 (Figure 2D, 8 ± 1 polyps per mouse for Wip1 null/*Apc*$^{Min/+}$ compared to 67 ± 5 polyps per mouse for WT/*Apc*$^{Min/+}$, $p < 0.001$). Moreover, Wip1 null/*Apc*$^{Min/+}$ mice that survived beyond 300 days developed only 18 ± 1 polyps per mouse, which was statistically insignificant from the number of polyps developed by day 120 (8 ± 1 polyps per mouse). Polyp analysis showed that Wip1 null/*Apc*$^{Min/+}$

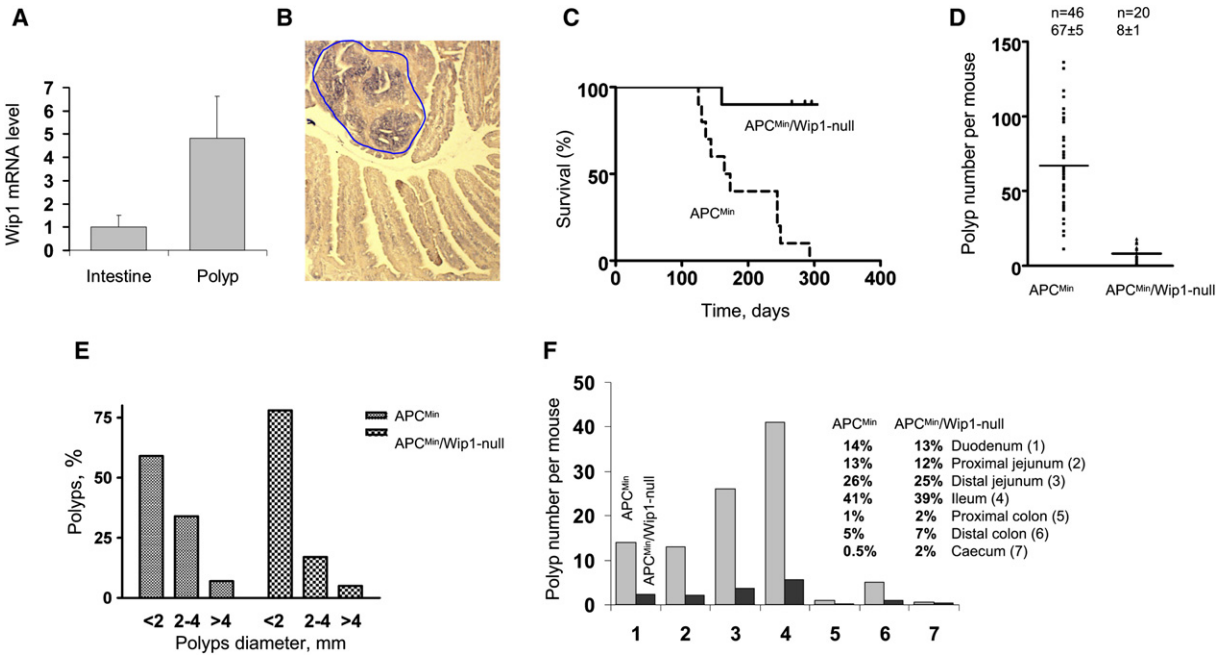


**Figure 2. Wip1 Phosphatase Regulates APC$^{Min}$-Induced Polyposis**

(A) Expression of Wip1 mRNA in normal intestinal epithelium and in microdissected polyps was analyzed using quantitative real-time PCR.

(B) Wip1 mRNA levels were analyzed using in situ hybridization in APC$^{Min}$ mice. The polyp area is outlined.

(C) Survival of APC$^{Min}$ and APC$^{Min}$/Wip1 null mice over a period of 300 days.

(D) The number of polyps in APC$^{Min}$ and APC$^{Min}$/Wip1 null mice at 120 days.

(E) The size distribution of polyps in APC$^{Min}$ and APC$^{Min}$/Wip1 null mice at 120 days.

(F) The distribution of polyps in APC$^{Min}$ and APC$^{Min}$/Wip1 null mice in different compartments of the mouse intestine.

polyps were smaller in size than WT/*Apc*$^{Min/+}$ polyps ($p = 0.05$) and were primarily localized to the small intestine (Figures 2E and 2F). Thus, Wip1 deficiency dramatically suppresses polyp formation in the presence of the *Apc*$^{Min}$ mutation, supporting the idea that Wip1 is critical in regulating *Apc*$^{Min}$-driven polyposis.

## Increased Intestinal Stem Cell Apoptosis in Wip1 Null Mice

Activation of the β-catenin signaling pathway is critical for polyp development through Tcf/Lef-dependent gene regulation (Korinek et al., 1997; Morin et al., 1997). To determine whether β-catenin activation was impaired in Wip1 null mice, immunohistochemical analysis was used to determine its subcellular localization. Although polyps that developed in Wip1 null/*Apc*$^{Min/+}$ mice were substantially smaller than in WT/*Apc*$^{Min/+}$ mice (Figure 3A, top panels), β-catenin was detected in the nuclei of polyp cells of both genotypes (Figure 3A, bottom panels). This suggests that Wip1 deficiency does not affect nuclear accumulation of β-catenin. Once β-catenin accumulates in the nucleus, it induces the transcription of Tcf/Lef-dependent genes. We observed increased expression of these genes in the intestines of *Apc*$^{Min/+}$ mice compared to wild-type mice (Figure 3B). A similar increase in mRNA levels for c-*myc*, cyclin D1, CD44, and Brachyury was found in Wip1 null/*Apc*$^{Min/+}$ compared to Wip1 null intestines, with no apparent difference between WT/*Apc*$^{Min/+}$ and wild-type mice, respectively. Thus, deficiency of Wip1 does not affect the β-catenin-Tcf/Lef-dependent signaling pathway.

Wip1 null mice show a profound tumor-resistant phenotype in several mouse models of cancer (Bulavin et al., 2004; Shreeram et al., 2006b). To determine how polyp formation is suppressed in Wip1 null/*Apc*$^{Min/+}$ mice (Figure 2D), we next analyzed cell proliferation and apoptosis in the intestine. Analysis of cell proliferation based on BrdU incorporation experiments revealed no difference between Wip1 null/*Apc*$^{Min/+}$ and WT/*Apc*$^{Min/+}$ mice where proliferative cells were restricted to the crypt compartment in both genotypes (Figure 3C). Similar results were obtained with another marker of proliferation, Ki-67 (data not shown). We also observed similar migration of BrdU-pulse-labeled epithelial cells in both WT/*Apc*$^{Min/+}$ and Wip1 null/*Apc*$^{Min/+}$ mice (data not shown). Analysis of apoptosis using an antibody to the active form of caspase-3 revealed positively stained cells in positions 4–6 from the base of the crypt in Wip1 null/*Apc*$^{Min/+}$ mice, while only a few positive cells were observed in WT/*Apc*$^{Min/+}$ mice (Figures 4A and 4B).

Self-renewal and organ development assays are not possible in the intestine as they are in other organs such as breast, prostate, or the hematopoietic system; however, the spatial organization of intestinal stem cells is well defined and documented (Potten and Ellis, 2006; Marshman et al., 2002; Clevers, 2006). A series of elegant experiments

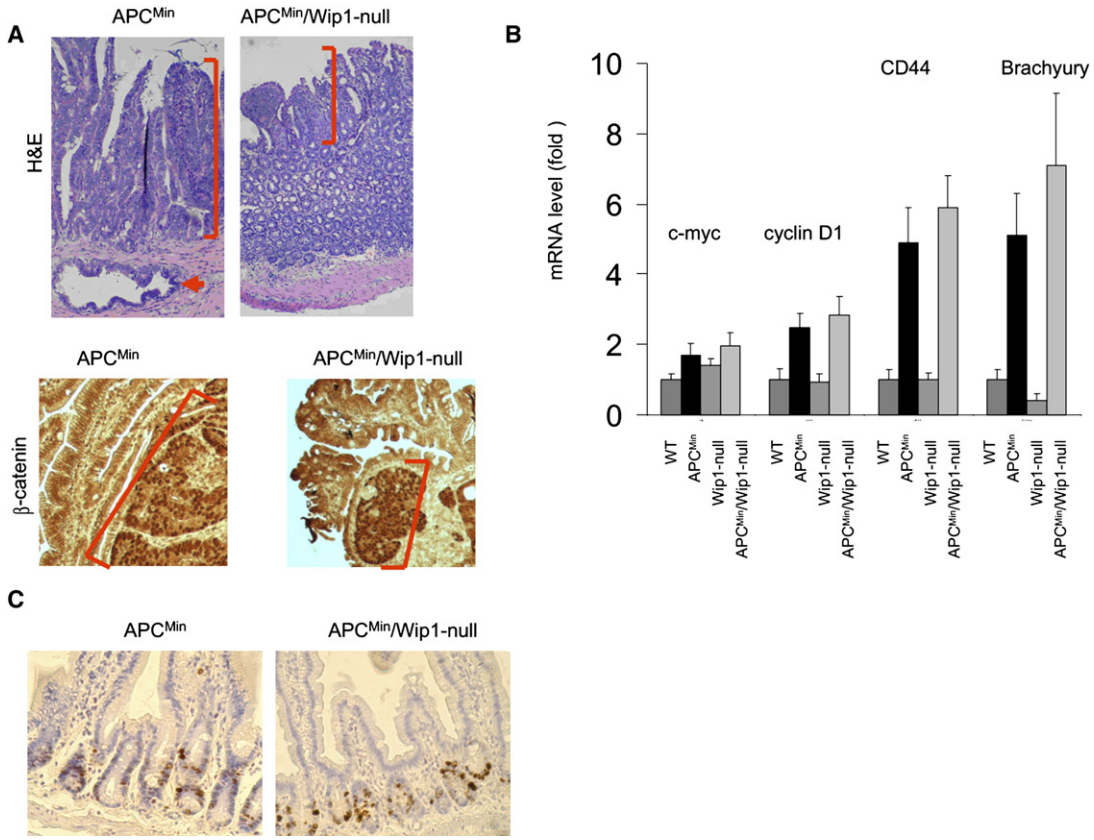


**Figure 3. Wip1 Deficiency Does Not Affect β-Catenin Signaling or Intestinal Cell Proliferation**

(A) Polyps from $APC^{Min}$ and $APC^{Min}$/Wip1 null mice at 120 days were analyzed after staining with hematoxylin and eosin (H&E; area of intramuscular tumor growth is shown with arrowhead) or with anti-β-catenin antibody (bottom panels). Nuclear staining was observed for β-catenin in the polyps of both $APC^{Min}$ and $APC^{Min}$/Wip1 null mice.

(B) mRNA levels of Tcf/Lef-dependent genes were analyzed in the intestines of wild-type, $APC^{Min}$, Wip1 null, and $APC^{Min}$/Wip1 null mice using real-time PCR. Error bars represent the standard deviation of triplicate experiments.

(C) Intestinal epithelium proliferation was analyzed after a 2 hr pulse with BrdU.

confirmed that intestinal stem cells are located in positions 4–6 from the base of the crypt, and several markers were characterized in these cells, including phospho-PTEN, Sox4, and Ascl2 (He et al., 2004; Van der Flier et al., 2007). As we found apoptotic cells in positions 4–6 in Wip1 null mice (Figure 4A and Figure S2), we next carried out double labeling to analyze markers of apoptosis and markers of intestinal stem cells, Sox4 and Ascl2, by RNA in situ hybridization (Figures 4D and 4E and Figure S2). We also used immunohistochemistry to analyze whether TUNEL-positive cells colocalized with another marker of intestinal stem cells, phospho-PTEN (Figure 4C). We found that ~80% of apoptosis-positive cells showed costaining with either Sox4, Ascl2, or phospho-PTEN. We next counted the number of positive cells for different markers according to their position along the crypt axis, as previously described (Potten et al., 2002). The cell position frequency plot showed that stem cell markers such as Sox4, Ascl2, and phospho-PTEN, as well as apoptotic cells analyzed in sections from Wip1 null mice, peaked at cell position 4 (Figures 1B, 4A, 4D, and 4E). Similar frequency plots were obtained for stem cell markers in wild-type mice (data not shown).

To unambiguously confirm that some intestinal stem cells undergo apoptosis in Wip1 null mice, we carried out a label-retaining experiment using juvenile mice (Potten et al., 2002). We found that cells undergoing apoptosis also retained [$^3$H]thymidine (Figure 4F). These data strongly support the idea that intestinal stem cells in Wip1 null/$Apc^{Min/+}$ mice undergo apoptosis. Consistent with the hypothesis that some intestinal stem cells reside in the Paneth area (Bjerknes and Cheng, 2006), we found that about 40% of cells in the Paneth cell compartment are reactive for the stem cell markers Sox4, Ascl2, and phospho-PTEN, retain [$^3$H]thymidine, and undergo apoptosis in Wip1 null mice (Figure 4).

There is a low level of spontaneous apoptosis of intestinal stem cells in $APC^{Min}$-Wip1 null mice (Figures 4A and 4B). This is different from a massive cell death of intestinal stem cells after IR, which leads to a compensatory increase in the number of proliferative cells in the crypt compartment (Potten et al., 1995). In turn, the death of a few intestinal stem cells, as in Wip1 null mice (Figures 4A and 4B), is not detrimental to the function of the particular crypt as these cells could be easily replaced with either

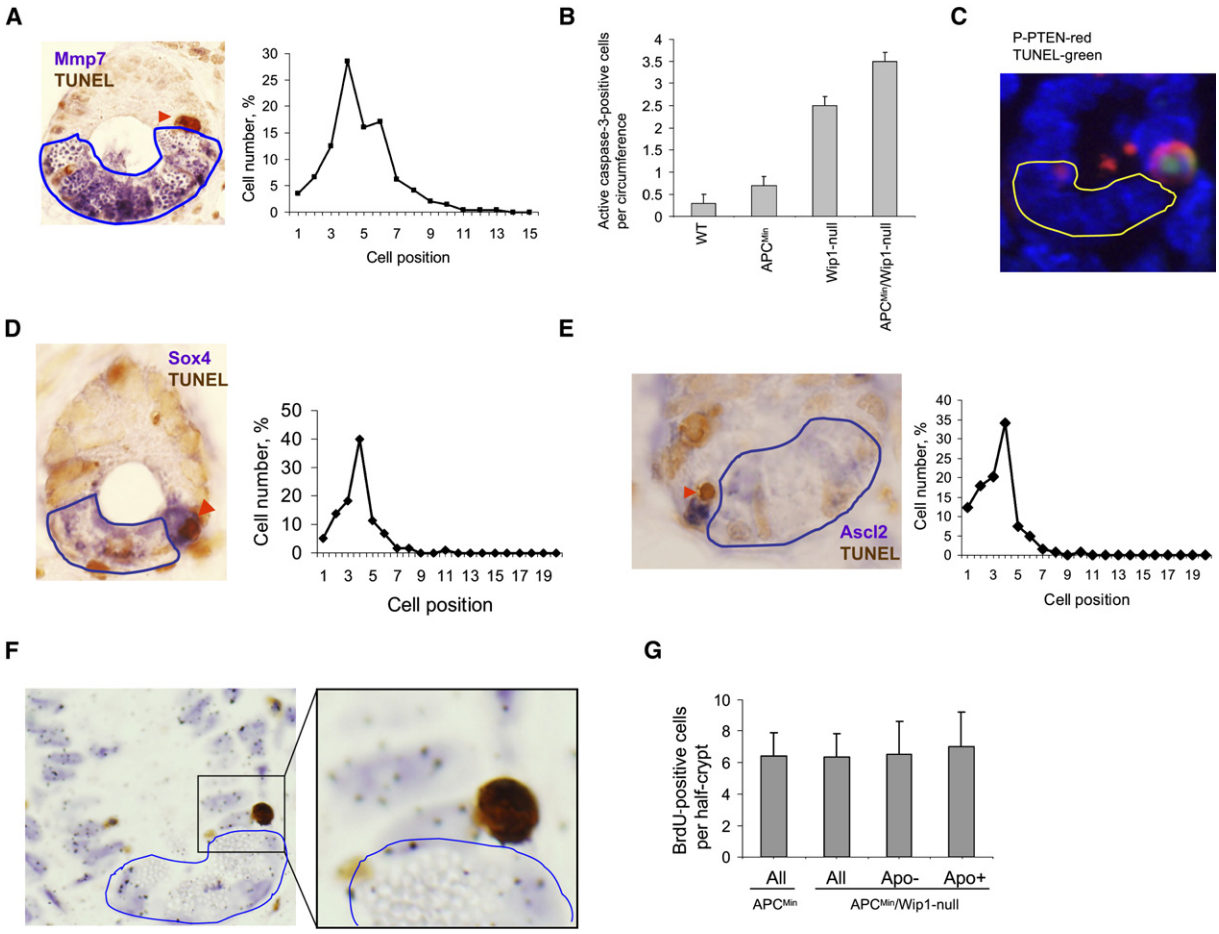


**Figure 4. Wip1 Deficiency Results in Intestinal Stem Cell Apoptosis**

Apoptosis in the intestines of mice was detected using either the TUNEL assay ([A], indicated with arrowhead) or an antibody to active caspase-3 (B). The Paneth cells were counterstained using RNA in situ hybridization to visualize MMP7. Cross-sections of intestines from $APC^{Min}$/Wip1 null mice were analyzed for stem cell markers phospho-PTEN (C), Sox4 (D), or Ascl2 (E). Apoptotic cells were stained with TUNEL (indicated with arrowheads). The area containing Paneth cells was identified based on the visual identification of cell-specific granules and is outlined on each image. (F) Label-retaining experiments were carried out with juvenile Wip1 null mice, and slides were counterstained for apoptosis. High-magnification figure (right panel) shows a TUNEL-positive cell in position 4 containing multiple grains of incorporated [$^3$H]thymidine. (G) Wild-type and Wip1 null mice were pulse labeled with BrdU, and the numbers of BrdU-positive cells in the crypts that either had or did not have apoptotic stem cells were counted. Apo (–) stands for crypts without apoptotic stem cells; Apo (+) stands for crypts with apoptotic stem cells. At least 50 crypts were counted for each group. (B and G) Error bars represent the standard deviation of triplicate experiments.

early proliferative progenitors or another stem cell (discussed below). Thus, it is conceivable to see no compensation in proliferation in the crypt progenitor compartment of Wip1 null intestine (Figure 3C). To further verify this, we counted BrdU-positive cells in the crypts that either had or did not have apoptotic stem cells in Wip1 null mice and compared the numbers with wild-type mice. As shown in Figure 4G, we found no difference in the number of BrdU-positive cells between different groups.

## p53 Tumor Suppressor Protects Wip1 Null Mice from $APC^{Min}$-Induced Polyposis

To investigate the molecular mechanisms that cause Wip1 null mice to be resistant to $Apc^{Min}$-driven polyposis, we investigated the expression of cell-cycle control/apoptosis proteins in extracts from the intestines of mice with different genotypes (Figure 5A). While no difference was observed in expression of β-catenin, Cox-2, $p27^{Kip1}$, $p16^{Ink4a}$, $p19^{Arf}$, and cyclin D1 between WT/$Apc^{Min/+}$ (lane 2) and Wip1 null/$Apc^{Min/+}$(lane 4) intestines, the level of expression of the p53 tumor suppressor and its downstream target, $p21^{Waf1}$, was increased in Wip1 null tissues. To understand the contribution of p53 to $p21^{Waf1}$ activation, we next crossed Wip1 null/$Apc^{Min/+}$ mice with p53 null mice, and subsequently intercrossed either p53-het/$Apc^{Min/+}$ or Wip1 null/p53-het/$Apc^{Min/+}$ mice, to yield four genotypes: $Apc^{Min/+}$ and p53 null/$Apc^{Min/+}$; Wip1 null/$Apc^{Min/+}$ and Wip1 null/p53 null/$Apc^{Min/+}$. Next, we purified intestinal crypts from 8- to 12-week-old mice, confirmed the presence of the crypt base by analyzing lysozyme-positive (Paneth) cells (Figure S1), and analyzed protein expression by western blotting. We found that

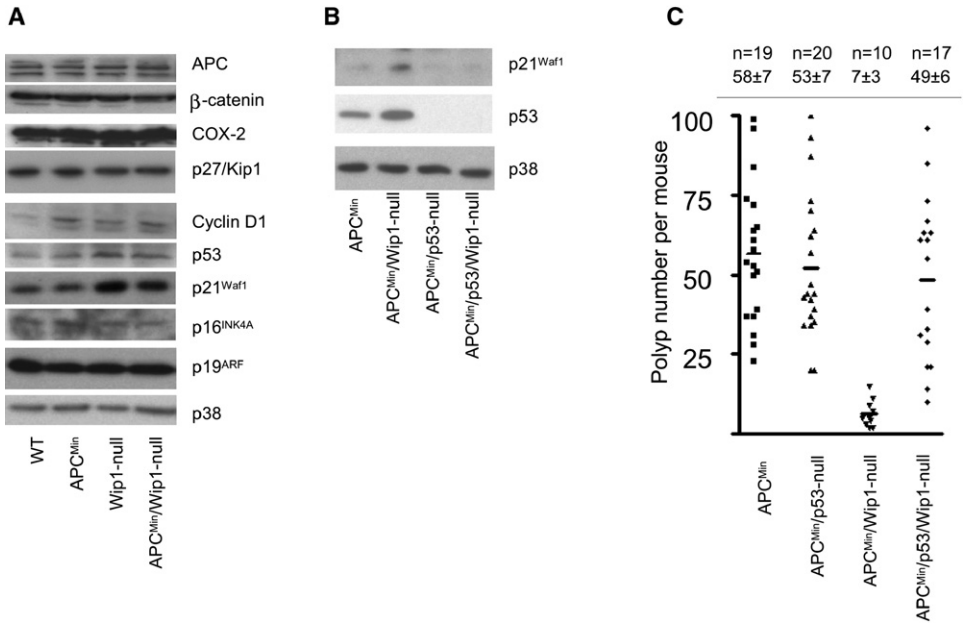


**Figure 5. The p53-Dependent Signaling Pathway Is Critical for Resistance to Polyposis in Wip1 Null Mice**

(A) The indicated antibodies were used to analyze proteins in extracts from the ileums of wild-type, $APC^{Min}$, Wip1 null, and $APC^{Min}$/Wip1 null mice.

(B) Protein expression was analyzed in intestinal crypts purified from 4- to 6-week-old $APC^{Min}$, $APC^{Min}$/Wip1 null, $APC^{Min}$/p53 null, and $APC^{Min}$/p53 null/Wip1 null mice.

(C) The number of polyps in $APC^{Min}$, $APC^{Min}$/p53 null, and $APC^{Min}$/p53 null/Wip1 null mice were counted at 90 days.

both p53 and $p21^{Waf1}$ were upregulated (~2 and 6 fold, respectively) in epithelial cells obtained from Wip1 null/$Apc^{Min/+}$ mice compared to WT/$Apc^{Min/+}$ mice (Figure 5B). In turn, removal of p53 eliminated the difference in $p21^{Waf1}$ expression levels between the different genotypes, supporting the idea that expression of $p21^{Waf1}$ is regulated in a p53-dependent manner in Wip1 null intestinal epithelium.

To understand the contribution of p53-dependent signaling pathways in suppressing $Apc^{Min}$-driven polyposis in Wip1 null mice, we next analyzed polyp formation in mice of different genotype: $Apc^{Min/+}$ and p53 null/$Apc^{Min/+}$ (one group of littermates), Wip1 null/$Apc^{Min/+}$ and Wip1 null/p53 null/$Apc^{Min/+}$ (another group of littermates). For this set of experiments, we counted polyps at 90 days, because the majority of p53 null mice rapidly succumb to cancer (primarily lymphomas) later in life (Donehower et al., 1992). We found that the deletion of p53 caused an outbreak of polyp formation in Wip1/p53 null/$Apc^{Min/+}$ mice (49 ± 6 polyps for Wip1/p53 null/$Apc^{Min/+}$ versus 7 ± 3 polyps per mouse for Wip1 null/$Apc^{Min/+}$ mice [Figure 5C]). Thus, p53 is important in rendering Wip1 null mice resistant to polyposis.

## Activation of Wnt-Dependent Signaling Drives Apoptosis of Wip1 Null Intestinal Stem Cells

The p53 tumor suppressor plays a primary role in regulating cell-cycle arrest and apoptosis (Wilson et al., 1998; Christophorou et al., 2006; Oren, 2001). In turn, activation of p53 could sensitize intestinal stem cells to DNA damage-induced apoptosis caused by IR, which would explain why intestinal stem cells are efficiently killed in a p53-dependent manner at a dose as low as 0.01 Gy of IR (Ishizuka et al., 2003). Homozygous loss of wild-type APC results in constitutive activation of the Wnt/β-catenin signaling pathway; this could trigger, as does IR, an efficient p53 response that promotes apoptosis (Damalas et al., 1999; Sansom et al., 2004). To investigate how activation of β-catenin signaling modulates stem cell behavior, we next treated WT/$Apc^{Min/+}$ and Wip1 null/$Apc^{Min/+}$ mice with specific inhibitors of GSK, a kinase that induces phosphorylation-dependent degradation of β-catenin (Salic et al., 2000). In both genotypes, inactivation of GSK with different chemical inhibitors resulted in upregulation of Tcf/Lef-dependent genes such as cyclin D1 ($p = 0.026$), myc ($p = 0.042$), and CD44 ($p = 0.033$) (Figure 6A). Further analysis revealed that the intestinal stem cells of Wip1 null/$Apc^{Min/+}$ mice exhibited significant apoptosis after treatment with GSK inhibitors IX ($p = 0.021$), X ($p = 0.016$), and XIII ($p = 0.042$), while no changes were observed in WT/$Apc^{Min/+}$ mice (Figure 6B). Furthermore, both spontaneous apoptosis and GSK inhibitor IX-induced apoptosis of stem cells were completely abrogated after deletion of p53 in Wip1 null/$Apc^{Min/+}$ mice (Figure 6B). Similar results were obtained with GSK inhibitors X and XIII (data not shown). These data further support the idea that activation of the β-catenin signaling pathway triggers efficient apoptosis of intestinal stem cells under conditions in which the level of p53 is already attenuated, as in Wip1 null mice.

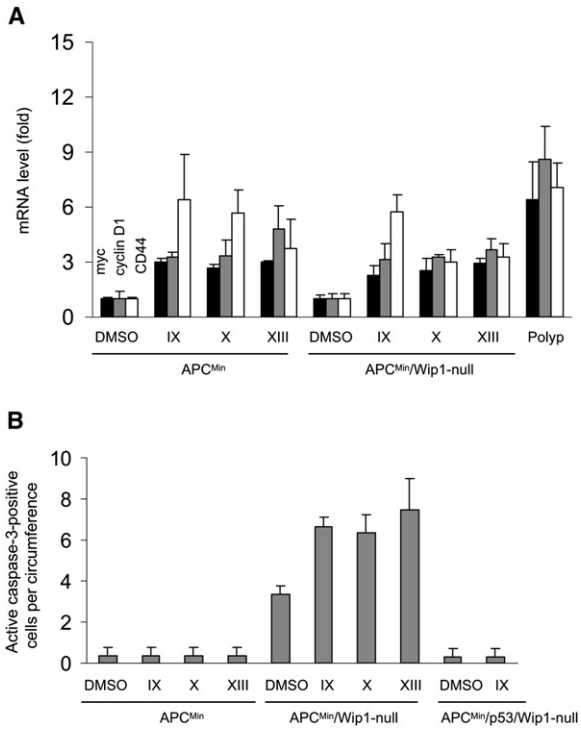


**Figure 6. Constitutive Activation of β-Catenin Signaling Results in Apoptosis of Intestinal Stem Cells in Wip1 Null Mice**

(A) WT/*Apc*$^{Min/+}$ and Wip1 null/*Apc*$^{Min/+}$ mice were injected with three different inhibitors of GSK (IX, X, and XIII, Calbiochem), and the level of expression of TCF/Lef-dependent genes was analyzed 10 hr later by real-time PCR.

(B) Analysis of apoptosis in the intestine of different genotypes 6 hr after injection of GSK inhibitor IX was carried out using an antibody to active caspase-3.

Error bars represent the standard deviation of triplicate experiments.

## DISCUSSION

The architecture of the intestine represents a unique anticancer barrier, as potential tumor-promoting DNA lesions caused by carcinogens and/or mutagens (consumed with food or by-products from bacterial load) do not pose a threat of tumor formation (Potten and Ellis, 2006). These damaged cells are efficiently removed from the intestine due to the continuous flow of epithelial cells from the base of the crypt to the tip of the villus (Clevers, 2006). Intestinal stem cells, which are located in positions 4–6 from the crypt base and in the Paneth area (Potten et al., 2002; Potten and Ellis, 2006; Bjerknes and Cheng, 2006), are the only type of continuously dividing cell that escapes this flow. Thus, it is conceivable that molecular changes that ultimately contribute to CRC may originate within these cells (Sancho et al., 2004). The stem cell origin of CRC is further supported by the fact that several intestinal stem cell markers were found to be abundant in APC$^{Min}$ adenomas and carcinomas (Van der Flier et al., 2007). Once a stem cell acquires a cancer-promoting genetic change, however, it is converted into a cancer stem cell that subsequently gives rise to polyps and, eventually, to more advanced cancers.

Accumulating evidence supports the role of stem cells in tumorigenesis (Leedham et al., 2005; O'Brien et al., 2007; Ricci-Vitiani et al., 2007). This would ultimately require their conversion into cancer stem cells in the course of tumorigenesis, a task that stem cells are prohibited to fulfill due to their nature. Stem cells, and intestinal stem cells in particular, while dividing continuously during their lifespan, show little evidence of any decline in the proliferation potential yet rarely develop carcinogenic mutations, suggesting that their genome is extremely well protected (Potten et al., 2002). This protection is achieved by several mechanisms, including their ability to selectively sort old (parental) and newly synthesized strands of DNA, a process called asymmetric division (Morrison and Kimble, 2006). If this mechanism fails, stem cells are further protected against acquiring changes in their genome by undergoing apoptosis when such errors occur (Potten et al., 2002). These two processes could be interconnected, as the inability to undergo efficient repair process (as a part of asymmetric division) could explain high sensitivity of stem cells to genotoxic damage because some repair enzymes would be common to both processes. In turn, modification of either mechanism could expedite tumorigenesis or serve as a powerful cancer-prevention tool, as demonstrated here in Wip1 null mice.

If cancer originates in a stem cell (Leedham et al., 2005; O'Brien et al., 2007; Ricci-Vitiani et al., 2007), certain genetic alterations observed in the early stages of cancer should be traceable back to a particular stem cell. In the case of the *APC*$^{Min}$-induced model of polyposis, *Apc*$^{+}$ allelic loss was detected in all lesions examined by Levy et al. (1994), who observed inactivation even in the earliest recognizable phase of tumors. Thus, the loss of the wild-type APC allele in *APC*$^{Min}$ mice that is observed in all polyps could originate in a single stem cell. In turn, once the stem cell acquires both mutant APC alleles, it will constitutively activate the β-catenin signaling pathway, triggering activation of Tcf/Lef-dependent genes as well as p53 (Damalas et al., 1999). Such activation of p53 in wild-type stem cells is well tolerated (Figure 6B); however, in a situation in which p53 is already elevated (as in Wip1 null cells), it induces apoptosis. Similarly, very small doses of radiation induce marked p53-dependent (ATM-independent) apoptosis, which is enhanced in a Wip1 null background, supporting the idea that intestinal stem cells are very sensitive to p53 activation (Merritt et al., 1994; Potten, 1977; Potten and Grant, 1998). Once a stem cell is destroyed, however, the asymmetric sister cells (the first or second early progenitor) replace it and assume the functions of a stem cell in repopulating the crypt (Martin et al., 1998). At this early stage in their lineage development, the asymmetric sister cells appear to retain stem cell properties (Potten and Ellis, 2006; Morrison and Kimble, 2006). Alternatively, symmetric division of a neighboring stem cell could replace a destroyed stem cell, because there are 4–6 stem cells per crypt (Potten and

Ellis, 2006; Marshman et al., 2002). The "self-destroying" mechanism, i.e., apoptosis, could be critical for preventing stem cells from converting into tumor-initiating/cancer stem cells and giving rise to intestinal cancer once the wild-type APC allele is lost and the β-catenin pathway is constitutively activated to drive polyposis. In conclusion, we show that the Wip1 phosphatase, which is highly expressed in the intestinal stem cells, regulates homeostasis of these cells, especially under stress conditions such as the presence of oncogenes. In turn, Wip1 loss suppresses $APC^{Min}$-driven polyposis by setting a threshold for p53-dependent apoptosis of stem cells, thus preventing their conversion into tumor-initiating stem cells.

## EXPERIMENTAL PROCEDURES

### Mouse Strains

All animal protocols used in this study were approved by the Institute of Molecular and Cell Biology Animal Safety and Use Committee. Wip1 null (129Sv-C57BL/6 background) and p53 null (C57BL/6 background) mice were previously described (Donehower et al., 1992; Choi et al., 2002). $APC^{Min}$ heterozygous (C57BL/6J background) mice were obtained from the Jackson Laboratory. We crossed $Wip1^{+/-}$ mice with $APC^{Min}$ and $p53^{+/-}$ mice to obtain mice of different genotypes. Mice were euthanized and polyps were counted at 90, 120, and 300 days.

### Immunohistochemistry

Formalin-fixed paraffin-embedded mouse intestinal samples were sectioned at 5 μm and mounted on coated slides. Following dewaxing and hydration, sections were pretreated with peroxidase blocking buffer (3% $H_2O_2$ in methanol) for 20 min at room temperature (RT). Antigen retrieval was performed by autoclaving samples in Na-citrate buffer (10 mM, pH 6.0) for 30 min. Blocking of nonspecific binding was performed using 3% BSA or 5% blocking reagent (Roche) for 30 min at RT. All antibodies were incubated overnight at 4°C. The following antibodies were used: rabbit anti-lysozyme (1:150; DAKO); rabbit anti-caspase-3 (1:300) (AF835 R&D); anti-Wip1 antibody (Fujimoto et al., 2006); anti-p-PTEN (Ser380) antibody (1:25) (Cell Signaling Technology, Danvers, MA, USA); and goat anti-β-catenin (1:50; Santa Cruz, C-18). The BrdU staining kit (Zymed) and In Situ Cell Death Detection Kit (Roche) were used for BrdU staining and TUNEL assay, respectively. In all cases, the Envision+ kit (DAKO) was used as a secondary reagent. For goat anti-β-catenin antibodies, a bridge step using rabbit anti-goat antibodies was required. Staining was developed using DAB and counterstaining with hematoxylin.

For simultaneous staining of BrdU and active caspase-3, formalin-fixed tissue sections were deparaffined by passing through Xylene, 10 min × 3; 100% ethanol, 2 min × 2; 95% ethanol, 2 min × 1; 70% ethanol, 2 min × 1; and distilled water, 2 min × 3. Unmasking of epitope was accomplished using 10 mM citrate buffer (pH 6.0) at 121°C for 20 min in autoclave and subsequent DNase I (20 U/ml, NEB, Beverly, MA, USA) treatment for 30 min at 37°C. After DNase treatment, sections were washed with PBS, blocked with 2% BSA/PBS, and incubated with primary mouse monoclonal antibodies against BrdU (1:50) (BD Biosciences, San Jose, CA, USA) and rabbit polyclonal against active form of caspase-3 (1:200) (R&D Systems [AF835], Minneapolis, MN, USA) overnight at 4°C. After three washes with PBS, secondary anti-mouse Alexa 594 and anti-rabbit Alexa 488 antibodies (1:500) (Invitrogen Molecular Probes, Eugene, OR, USA) were applied for 1 hr at RT.

For simultaneous staining of TUNEL and PTEN, Carnoy's fixed tissue sections were deparaffined and microwaved in 100 mM citrate buffer (pH 6.0) at low power level for 4 min and rinsed three times with PBS, and TUNEL-positive cells were visualized with In Situ Cell Death Detection Kit (Fluorescein) (Roche Applied Bioscience, Manheim, Germany). Sections were washed three times with PBS, blocked with 2% BSA/PBS, and incubated with anti-p-PTEN (Ser380) antibody (1:25) (Cell Signaling Technology, Danvers, MA, USA) overnight at 4°C. After three washes with PBS, secondary anti-rabbit-Alexa 594 antibodies (1:500) (Invitrogen Molecular Probes, Eugene, OR, USA) were applied for 1 hr at RT. Vectashield mounting media with DAPI (Vector-Laboratories, Burlingame, CA, USA) was used to mount slides for subsequent analysis by Olympus BX61 microscope.

### In Situ mRNA Hybridization

Partial Mmp7, Ascl2, and Sox4 cDNAs were obtained by RT-PCR from total mouse RNA, and T7 promoter was added by additional PCR (primer sequences are available upon request). Probes were synthesized by in vitro transcription using MEGAscript T7 kit (Ambion) and DIG RNA labeling mix (Roche). Formalin-fixed paraffin-embedded mouse intestinal samples were sectioned at 5 μm and mounted on coated slides. Following standard dewaxing and hydration, samples were treated with 0.2 N HCl for 20 min at RT. The RNA in situ hybridization was performed using the mRNA Locator Kit (Ambion) protocol. Dig-labeled cRNA probes (500 ng/ml) were diluted in hybridization solution and hybridization was performed during 48 hr at 68°C. Detection of probe was achieved with sheep anti-digoxigenin Fab (Roche) conjugated to alkaline phosphatase (1/5000 in PBS/blocking powder; overnight at 4°C). Alkaline phosphatase activity was revealed with NBT/BCIP.

### Real-Time RT-PCR

mRNA expression was determined by real-time-PCR. Tissues were frozen in dry ice, and RNA was extracted using the TRIzol reagent (Invitrogen). Reverse transcription was performed using Superscript II (Invitrogen) according to the manufacturer's instructions. Real-time PCR was performed by LightCycler 2.0 Real-Time PCR System (Roche) with LightCycler FastStart DNA MasterPlus SYBR Green I (Roche). GAPDH and HRPT mRNA levels were used as a reference. Primers were designed using the Primer3 program (Rozen and Skaletsky, 2000). Ppm1d 5′-CAGAAAGGCTTCACCTCGTC-3′; 5′-CACCTCCACAGCTCTCACAA-3′. Brachyury 5′-TCCCGAGACCCAGTTCATAG-3′ and 5′-TGACCGGTGGTTCCTTAGAG-3′; Ccn1d 5′-ACCGCACAACGCACTTTCT-3′ and 5′-TCCACATCTCGCACGTCGGT-3′; CD44 5′-CTCTCCTGGCACTGGCTCTGATTC-3′ and 5′-GTCCGGGGTCTCTGATGGTTCC-3′. c-*myc* 5′-AGCTCGCCCAAATCCTGTA-3′ and 5′-AGCCCGACTCCGACCTCT-3′.

### GSK-3 Inhibition

Mice were injected i.p. with the GSK-3 inhibitors IX, X, and XII (Calbiochem, 361550), 15 mg per kg of body weight in 5% DMSO. After 6 hr and 10 hr, mice were euthanized and organs were collected for subsequent analysis.

### Isolation of Intestinal Crypts

Small intestinal crypts were isolated from adult male mice of 6–12 weeks (Booth et al., 1999; Grossmann et al., 1998). The intestinal segments were isolated, the lumenal contents were flushed out with PBS, and the tissue was slit open longitudinally. After chopping into ~5 mm pieces, the fragments were washed three times in PBS, 1 time in 10 mmol/l dithiothreitol/PBS (Sigma Chemical Co., St. Louis, MO, USA) for 20 min and one time in 1 mmol/l EDTA (Sigma Chemical Co., St. Louis, MO, USA) for 20 min. Epithelial cells were detached as intact crypts and villus by ten vigorous shakes of the vessel. Large pieces of intestine were then allowed to settle under gravity for 1 min, leaving the isolated crypts and villus in suspension. These were removed and retained. The sedimented pellet was shaken vigorously to release further crypts, resuspended in 45 ml PBS, and then allowed to settle under gravity again. The suspended crypts and villus were pooled with the original retained sample and then centrifuged at 300 rpm in a Sorvall Legend RT centrifuge. The step was repeated three times until the supernatant appeared clear. The purified intestinal

epithelial cells were divided into two parts. The first part was used for protein extraction, subsequent electrophoresis, and western blotting with antibody against $p21^{Waf1}$, p53, and p38. The remaining material was fixed in 4% paraformaldehyde for 1 hr at 4°C, permeabilized using 0.5% Triton X-100 in PBS, and used for whole-mount immunofluorescent staining with anti-lysozyme antibody.

### Label-Retaining Experiments

We performed juvenile labeling on mice aged between 36 and 45 days postnatum (Potten et al., 2002). Mice were injected with 50 μCi [$^3$H]thymidine (Amersham) i.p. twice daily for three consecutive days. All animals were sacrificed 21 days after last injection. The intestinal tissue was fixed (Carnoy's and formalin). Sections were first immunohistochemically stained for Wip1, active caspase-3, or TUNEL. Autoradiography was undertaken using K5 emulsion (Ilford Photo, Cheshire, UK). The threshold for detecting label-retaining cells was set at ten or more grains per nucleus.

### Statistical Analysis

To assess the statistical significance of the results, each experiment was repeated at least three times, means and standard deviations between different groups were calculated, and error bars were included where necessary. Student's t test was performed for paired analysis. Kaplan-Meier analysis of survival was performed with the assistance of PRISM4 statistical analysis software.

### Supplemental Data

Supplemental Data include two figures and can be found with this article online at http://www.cellstemcell.com/cgi/content/full/1/2/180/DC1/.

## ACKNOWLEDGMENTS

This work was supported by the Agency for Science, Technology and Research (Singapore). The research for E.A. was supported by the Intramural Research Program of the National Institutes of Health, National Cancer Institute. We would like to acknowledge the support by Dr. A.J. Fornace, Jr., with the $APC^{Min}$ model approach.

Received: January 3, 2007
Revised: April 19, 2007
Accepted: May 31, 2007
Published: August 15, 2007

## REFERENCES

Bjerknes, M., and Cheng, H. (2006). Intestinal epithelial stem cells and progenitors. Methods Enzymol. *419*, 337–383.

Booth, C., O'Shea, J.A., and Potten, C.S. (1999). Maintenance of functional stem cells in isolated and cultured adult intestinal epithelium. Exp. Cell Res. *249*, 359–366.

Bulavin, D.V., Phillips, C., Nannenga, B., Timofeev, O., Donehower, L.A., Anderson, C.W., Appella, E., and Fornace, A.J., Jr. (2004). Inactivation of the Wip1 phosphatase inhibits mammary tumorigenesis through p38 MAPK-mediated activation of the p16(Ink4a)-p19(Arf) pathway. Nat. Genet. *36*, 343–350.

Choi, J., Nannenga, B., Demidov, O.N., Bulavin, D.V., Cooney, A., Brayton, C., Zhang, Y., Mbawuike, I.N., Bradley, A., Appella, E., and Donehower, L.A. (2002). Mice deficient for the wild-type p53-induced phosphatase gene (Wip1) exhibit defects in reproductive organs, immune function, and cell cycle control. Mol. Cell. Biol. *22*, 1094–1105.

Christophorou, M.A., Ringshausen, I., Finch, A.J., Swigart, L.B., and Evan, G.I. (2006). The pathological response to DNA damage does not contribute to p53-mediated tumour suppression. Nature *443*, 214–217.

Clevers, H. (2006). Wnt/beta-catenin signaling in development and disease. Cell *127*, 469–480.

Corpet, D.E., and Pierre, F. (2003). Point: from animal models to prevention of colon cancer. Systematic review of chemoprevention in min mice and choice of the model system. Cancer Epidemiol. Biomarkers Prev. *12*, 391–400.

Damalas, A., Ben Ze'ev, A., Simcha, I., Shtutman, M., Leal, J.F., Zhurinsky, J., Geiger, B., and Oren, M. (1999). Excess beta-catenin promotes accumulation of transcriptionally active p53. EMBO J. *18*, 3054–3063.

Demidov, O.N., Kek, C., Shreeram, S., Timofeev, O., Fornace, A.J., Appella, E., and Bulavin, D.V. (2007). The role of the MKK6/p38 MAPK pathway in Wip1-dependent regulation of ErbB2-driven mammary gland tumorigenesis. Oncogene *26*, 2502–2506.

Donehower, L.A., Harvey, M., Slagle, B.L., McArthur, M.J., Montgomery, C.A., Jr., Butel, J.S., and Bradley, A. (1992). Mice deficient for p53 are developmentally normal but susceptible to spontaneous tumours. Nature *356*, 215–221.

Fiscella, M., Zhang, H., Fan, S., Sakaguchi, K., Shen, S., Mercer, W.E., Vande Woude, G.F., O'Connor, P.M., and Appella, E. (1997). Wip1, a novel human protein phosphatase that is induced in response to ionizing radiation in a p53-dependent manner. Proc. Natl. Acad. Sci. USA *94*, 6048–6053.

Fujimoto, H., Onishi, N., Kato, N., Takekawa, M., Xu, X.Z., Kosugi, A., Kondo, T., Imamura, M., Oishi, I., Yoda, A., and Minami, Y. (2006). Regulation of the antioncogenic Chk2 kinase by the oncogenic Wip1 phosphatase. Cell Death Differ. *13*, 1170–1180.

Grossmann, J., Maxson, J.M., Whitacre, C.M., Orosz, D.E., Berger, N.A., Fiocchi, C., and Levine, A.D. (1998). New isolation technique to study apoptosis in human intestinal epithelial cells. Am. J. Pathol. *153*, 53–62.

He, X.C., Zhang, J., Tong, W.G., Tawfik, O., Ross, J., Scoville, D.H., Tian, Q., Zeng, X., He, X., Wiedemann, L.M., et al. (2004). BMP signaling inhibits intestinal stem cell self-renewal through suppression of Wnt-beta-catenin signaling. Nat. Genet. *36*, 1117–1121.

He, X.C., Yin, T., Grindley, J.C., Tian, Q., Sato, T., Tao, W.A., Dirisina, R., Porter-Westpfahl, K.S., Hembree, M., Johnson, T., et al. (2007). PTEN-deficient intestinal stem cells initiate intestinal polyposis. Nat. Genet. *39*, 189–198.

Ishizuka, S., Martin, K., Booth, C., Potten, C.S., de Murcia, G., Burkle, A., and Kirkwood, T.B. (2003). Poly(ADP-ribose) polymerase-1 is a survival factor for radiation-exposed intestinal epithelial stem cells in vivo. Nucleic Acids Res. *31*, 6198–6205.

Korinek, V., Barker, N., Morin, P.J., van Wichen, D., de Weger, R., Kinzler, K.W., Vogelstein, B., and Clevers, H. (1997). Constitutive transcriptional activation by a beta-catenin-Tcf complex in APC−/− colon carcinoma. Science *275*, 1784–1787.

Leedham, S.J., Thliveris, A.T., Halberg, R.B., Newton, M.A., and Wright, N.A. (2005). Gastrointestinal stem cells and cancer: bridging the molecular gap. Stem Cell Rev. *1*, 233–241.

Levy, D.B., Smith, K.J., Beazer-Barclay, Y., Hamilton, S.R., Vogelstein, B., and Kinzler, K.W. (1994). Inactivation of both APC alleles in human and mouse tumors. Cancer Res. *54*, 5953–5958.

Lu, X., Nannenga, B., and Donehower, L.A. (2005). PPM1D dephosphorylates Chk1 and p53 and abrogates cell cycle checkpoints. Genes Dev. *19*, 1162–1174.

Marshman, E., Booth, C., and Potten, C.S. (2002). The intestinal epithelial stem cell. Bioessays *24*, 91–98.

Martin, K., Potten, C.S., Roberts, S.A., and Kirkwood, T.B. (1998). Altered stem cell regeneration in irradiated intestinal crypts of senescent mice. J. Cell Sci. *111*, 2297–2303.

Merritt, A.J., Potten, C.S., Kemp, C.J., Hickman, J.A., Balmain, A., Lane, D.P., and Hall, P.A. (1994). The role of p53 in spontaneous and radiation-induced apoptosis in the gastrointestinal tract of normal and p53-deficient mice. Cancer Res. *54*, 614–617.

Morin, P.J., Sparks, A.B., Korinek, V., Barker, N., Clevers, H., Vogelstein, B., and Kinzler, K.W. (1997). Activation of beta-catenin-Tcf signaling in colon cancer by mutations in beta-catenin or APC. Science *275*, 1787–1790.

Morrison, S.J., and Kimble, J. (2006). Asymmetric and symmetric stem-cell divisions in development and cancer. Nature *441*, 1068–1074.

Nannenga, B., Lu, X., Dumble, M., Van Maanen, M., Nguyen, T.A., Sutton, R., Kumar, T.R., and Donehower, L.A. (2006). Augmented cancer resistance and DNA damage response phenotypes in PPM1D null mice. Mol. Carcinog. *45*, 594–604.

O'Brien, C.A., Pollett, A., Gallinger, S., and Dick, J.E. (2007). A human colon cancer cell capable of initiating tumour growth in immunodeficient mice. Nature *445*, 106–110.

Oren, M. (2001). The p53 saga: the good, the bad, and the dead. Harvey Lect. *97*, 57–82.

Polakis, P. (1997). The adenomatous polyposis coli (APC) tumor suppressor. Biochim. Biophys. Acta *1332*, F127–F147.

Potten, C.S. (1977). Extreme sensitivity of some intestinal crypt cells to X and gamma irradiation. Nature *269*, 518–521.

Potten, C.S., and Grant, H.K. (1998). The relationship between ionizing radiation-induced apoptosis and stem cells in the small and large intestine. Br. J. Cancer *78*, 993–1003.

Potten, C.S., and Ellis, J.R. (2006). Adult small intestinal stem cells: identification, location, characteristics, and clinical applications. Ernst Schering Res. Found. Workshop *60*, 81–98.

Potten, C.S., Owen, G., Hewitt, D., Chadwick, C.A., Hendry, H., Lord, B.I., and Woolford, L.B. (1995). Stimulation and inhibition of proliferation in the small intestinal crypts of the mouse after in vivo administration of growth factors. Gut *36*, 864–873.

Potten, C.S., Owen, G., and Booth, D. (2002). Intestinal stem cells protect their genome by selective segregation of template DNA strands. J. Cell Sci. *115*, 2381–2388.

Radtke, F., and Clevers, H. (2005). Self-renewal and cancer of the gut: two sides of a coin. Science *307*, 1904–1909.

Reitmair, A.H., Cai, J.C., Bjerknes, M., Redston, M., Cheng, H., Pind, M.T., Hay, K., Mitri, A., Bapat, B.V., Mak, T.W., and Gallinger, S. (1996). MSH2 deficiency contributes to accelerated APC-mediated intestinal tumorigenesis. Cancer Res. *56*, 2922–2926.

Ricci-Vitiani, L., Lombardi, D.G., Pilozzi, E., Biffoni, M., Todaro, M., Peschle, C., and De Maria, R. (2007). Identification and expansion of human colon-cancer-initiating cells. Nature *445*, 111–115.

Rozen, S., and Skaletsky, H.J. (2000). Primer3 on the WWW for general users and for biologist programmers. Methods Mol. Biol. *132*, 365–386.

Salic, A., Lee, E., Mayer, L., and Kirschner, M.W. (2000). Control of beta-catenin stability: reconstitution of the cytoplasmic steps of the wnt pathway in Xenopus egg extracts. Mol. Cell *5*, 523–532.

Sancho, E., Batlle, E., and Clevers, H. (2004). Signaling pathways in intestinal development and cancer. Annu. Rev. Cell Dev. Biol. *20*, 695–723.

Sansom, O.J., Reed, K.R., Hayes, A.J., Ireland, H., Brinkmann, H., Newton, I.P., Batlle, E., Simon-Assmann, P., Clevers, H., Nathke, I.S., et al. (2004). Loss of Apc in vivo immediately perturbs Wnt signaling, differentiation, and migration. Genes Dev. *18*, 1385–1390.

Shreeram, S., Demidov, O.N., Hee, W.K., Yamaguchi, H., Onishi, N., Kek, C., Timofeev, O.N., Dudgeon, C., Fornace, A.J., Anderson, C.W., et al. (2006a). Wip1 phosphatase modulates ATM-dependent signaling pathways. Mol. Cell *23*, 757–764.

Shreeram, S., Hee, W.K., Demidov, O.N., Kek, C., Yamaguchi, H., Fornace, A.J., Jr., Anderson, C.W., Appella, E., and Bulavin, D.V. (2006b). Regulation of ATM/p53-dependent suppression of myc-induced lymphomas by Wip1 phosphatase. J. Exp. Med. *203*, 2793–2799.

Su, L.K., Kinzler, K.W., Vogelstein, B., Preisinger, A.C., Moser, A.R., Luongo, C., Gould, K.A., and Dove, W.F. (1992). Multiple intestinal neoplasia caused by a mutation in the murine homolog of the APC gene. Science *256*, 668–670.

Urbanek, K., Cesselli, D., Rota, M., Nascimbene, A., De Angelis, A., Hosoda, T., Bearzi, C., Boni, A., Bolli, R., Kajstura, J., et al. (2006). Stem cell niches in the adult mouse heart. Proc. Natl. Acad. Sci. USA *103*, 9226–9231.

Van der Flier, L.G., Sabates-Bellver, J., Oving, I., Haegebarth, A., De Palo, M., Anti, M., Van Gijn, M.E., Suijkerbuijk, S., Van de Wetering, M., Marra, G., and Clevers, H. (2007). The intestinal Wnt/TCF signature. Gastroenterology *132*, 628–632.

Waikel, R.L., Kawachi, Y., Waikel, P.A., Wang, X.J., and Roop, D.R. (2001). Deregulated expression of c-Myc depletes epidermal stem cells. Nat. Genet. *28*, 165–168.

Welm, B.E., Tepera, S.B., Venezia, T., Graubert, T.A., Rosen, J.M., and Goodell, M.A. (2002). Sca-1(pos) cells in the mouse mammary gland represent an enriched progenitor cell population. Dev. Biol. *245*, 42–56.

Wilson, J.W., Pritchard, D.M., Hickman, J.A., and Potten, C.S. (1998). Radiation-induced p53 and p21WAF-1/CIP1 expression in the murine intestinal epithelium: apoptosis and cell cycle arrest. Am. J. Pathol. *153*, 899–909.